Journal of Solid State Chemistry **168,** 267–274 (2002)
doi:10.1006/jssc.2002.9721

Reversible Luminescence Thermochromism in Dipotassiumsodium Tris[dicyanoargentate(I)] and the Role of Structural Phase Transitions

P. Fischer,*,[1] B. Lucas,† M. A. Omary,‡ C. L. Larochelle,§ and H. H. Patterson¶

*Laboratory for Neutron Scattering, ETH Zurich & Paul Scherrer Institute, CH-5232 Villigen PSI, Switzerland; †Department of Physics, University of Queensland, Brisbane, Queensland 4072, Australia; ‡Department of Chemistry, University of North Texas, Denton, Texas 76203, USA; §Franklin & Marshall College, Lancaster, Pennsylvania 17604, USA; and ¶Department of Chemistry, University of Maine, Orono, Maine 04469, USA

Received April 19, 2002; in revised form June 24, 2002; accepted July 16, 2002

As a function of temperature, the layered compound $K_2Na[Ag(CN)_2]_3$ displays dramatic variations in luminescence thermochromism with major trend changes occurring around 80 K. In order to understand these interesting optical properties, high-resolution neutron diffraction investigations were performed on a polycrystalline sample of this material in the temperature range from 1.5 to 300 K, and previous synchrotron X-ray data of Larochelle *et al.* (*Solid State Commun.* 114, 155 (2000)) were reinterpreted. The corresponding significant structural changes were found to be continuous with an anomalous increase of the monoclinic *c*-lattice parameter with decreasing temperature, associated with slight reorientations of two inequivalent, approximately linear N–C–Ag–C–N units. In the whole temperature range, the crystal structure is monoclinic with the space group $C2/m$. Based on the structural results, the major luminescence thermochromism changes around 80 K are attributed to the dominance of a back energy transfer process from low- to high-energy excitons at high temperatures. © 2002 Elsevier Science (USA)

Key Words: **luminescence thermochromism; phase transitions; temperature dependence; crystal structure; neutron and synchrotron X-ray diffraction.**

1. INTRODUCTION

Luminescence thermochromism is an interesting optical phenomenon in which different emission colors are observed at different temperatures. There are only a few reported examples among molecular coordination compounds that show this phenomenon (1–5). The tetranuclear clusters $Cu_4L_4X_4$ (L =cyclic nitrogen base, X =halide) are the paramount examples of inorganic compounds showing luminescence thermochromism. The optical spectra of these clusters have been first reported by Hardt *et al.* (2) and the excited state assignment has been studied extensively, especially by Ford *et al.* (3) (for a review, see Ref. (3k)). More recently, however, other examples of luminescence thermochromism have been reported such as in trinuclear Au(I) compounds (4) and alkali–halide-doped $Ag(CN)_2^-$ crystals (5).

Here we describe interesting luminescence thermochromism results for the compound dipotassiumsodium tris [dicyanoargentate(I)], $K_2Na[Ag(CN)_2]_3$. The dramatic changes in the luminescence versus temperature merit a precise investigation of the crystal structure as a function of temperature. Subtle changes in Raman scattering have been detected in the compound $K_2Na[Ag(CN)_2]_3$ around 210 K (1). At room temperature, Zabel *et al.* published for $K_2Na[Ag(CN)_2]_3$ (6) a layer-type structure with approximately linear N–C–Ag–C–N groups. The angle N–C–Ag was reported as 176.7° instead of the chemically expected 180°. Trigonal symmetry according to space group $P\bar{3}1m$ had been determined by the authors from the single-crystal X-ray diffraction measurements. The bond distances Ag–C = 2.056(2) Å, C–N = 1.131(4) Å and Ag–N = 3.186(2) Å were found.

We have first performed high-resolution powder synchrotron X-ray and neutron diffraction studies at SNBL/ESRF and on D1A/ILL, Grenoble, respectively, in the temperature range from 1.5 to 300 K (1). The results indicated essential but continuous changes of the lattice parameters and, in particular, an anomalous increase of the *c*-lattice parameter with decreasing temperature. Moreover, the symmetry appeared in the whole temperature range to correspond to the monoclinic space group $C2/m$ rather than the trigonal space group $P\bar{3}1m$. Because of severe preferred orientation effects with a fixed sample in the neutron case and presumably due to limiting absorp-

[1] To whom correspondence should be addressed. Fax: 41-56-3102939. E-mail: peter.fischer@psi.ch.

0022-4596/02 $35.00

tion effects in the X-ray intensities dominated by Ag, we could not refine the structure properly. Because absorption is generally weak for neutrons and because neutron diffraction permits to locate in the presence of heavy atoms light atoms such as C and N precisely, we have carried out new high-resolution powder neutron diffraction investigations with an oscillating sample. Here we summarize the final refinement results on the temperature dependence of the structure of $K_2Na[Ag(CN)_2]_3$, which clearly prove that the space group $C2/m$ holds for this compound in the whole temperature range from 1.5 to 300 K. Prelimary results were reported in Ref. (7). In addition, we reinterpret the synchrotron X-ray data (1) with the neutron structure model of $K_2Na[Ag(CN)_2]_3$. On the basis of these results, conclusions are given about the origin of the temperature-dependent behavior of the optical properties of $K_2Na[Ag(CN)_2]_3$.

2. EXPERIMENTAL

The $K_2Na[Ag(CN)_2]_3$ compound was prepared based on the literature method, which entails the reaction of a stoichiometric mixture of NaCN, KCN, and AgCN in aqueous suspension followed by slow evaporation. Good-quality crystals of $K_2Na[Ag(CN)_2]_3$ were obtained. The compound is stable in air and light. Single crystals with good optical purity were chosen for the optical measurements using a microscope, while crystalline powders were used for the neutron diffraction studies.

Photoluminescence spectra were recorded with a model QuantaMaster-1046 fluorescence spectrophotometer from Photon Technology International, PTI. The instrument is equipped with two excitation monochromators and a 75 W xenon lamp. The spectra were recorded for single crystals with high optical purity as a function of temperature between 10 K and ambient temperature. Liquid helium was used as a coolant in a model LT3-110 Heli-Tran cryogenic liquid transfer system from Air Products equipped with a temperature controller.

The synchrotron X-ray measurements (1) were performed using a sample diameter of 0.5 mm (quartz glass capillary, rotating) and a wavelength of 0.79934 Å, yielding a calculated $\mu r = 0.336$ where μ and r are the linear absorption coefficient and sample radius, respectively. A powder density of 60% was assumed.

The neutron diffraction investigations were first (7) performed on instrument HRPT (8) at the Swiss continuous spallation neutron source SINQ of Paul Scherrer Institute, Villigen PSI on a powder sample of $K_2Na[Ag(CN)_2]_3$ in the temperature range from 9 to 300 K with the specimen in an oscillating CTI closed-cycle helium refrigerator. For this purpose, the sample was enclosed under He gas atmosphere into a cylindrical V container of 8 mm diameter and approximately 50 mm height, sealed by means of an indium wire. However, subsequent neutron diffraction measurements on HRPT with an oscillating ILL-type cryostat and temperatures in the range from 1.5 to 200 K showed that the previous CTI data suffered particularly at low temperatures from insufficient thermal contact of the cooled copper rod to the sample, yielding temperature gradients. Thus we summarize here the correct data and corresponding results. For the neutron diffraction investigations the wavelength $\lambda = 1.8856$ Å, primary collimation $\alpha_1 = 12'$, secondary collimation $\alpha_2 = 24'$ and the angular step $\delta(2\theta) = 0.05^\circ$ as well as scattering angles 2θ up to 165° were used. For the absorption correction $\mu r = 0.191$ was measured by transmission for the wavelength used. Profile analysis of the diffraction data was made by means of new versions of the program FullProf (9), based on the internal neutron scattering amplitudes, as well as by the program ZOMBIE (10), which is best adapted to introduce chemical molecular constraints. In the course of the refinements, corrections for preferred orientation according to the March function (9) appeared to be important, which are not yet implemented in program ZOMBIE. In the case of FullProf we used the Thompson–Cox–Hastings pseudo-Voigt peak shape (function 7) with a small Y parameter (9). In order to limit the number of parameters, we used the approximation of isotropic temperature factors. The background was fitted with a polynomial (six parameters).

3. PHOTOLUMINESCENCE SPECTRA

Figure 1 shows the emission spectra of single crystals of $K_2Na[Ag(CN)_2]_3$ at three selected temperatures. Two emission bands appear: a lower energy (LE) blue emission with a maximum near 410 nm and a higher energy (HE) ultraviolet emission with a maximum near 315 nm. Luminescence thermochromism is observed twice upon increasing the temperature from 10 K towards ambient

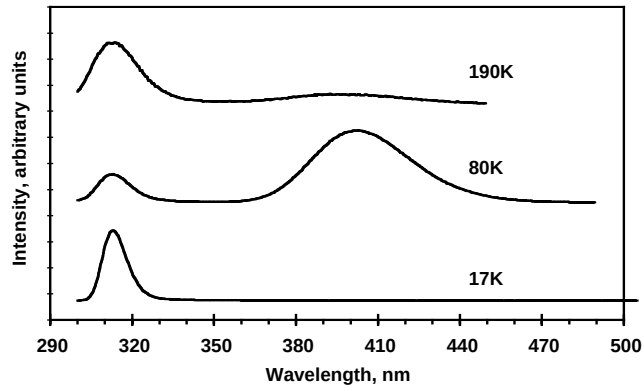

FIG. 1. Emission spectra of single crystals of $K_2Na[Ag(CN)_2]_3$ at three selected temperatures.

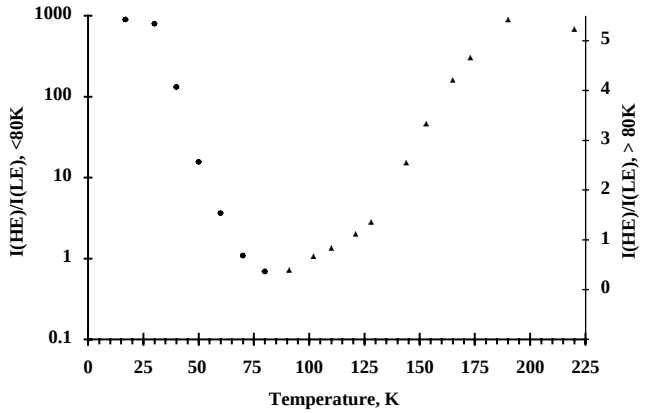

FIG. 2. A plot of the intensity ratio of the HE/LE emission bands of $K_2Na[Ag(CN)_2]_3$ versus temperature.

temperature. The HE band dominates at 10 K. Upon increasing the temperature, the LE band increases in intensity and becomes the dominant emission at 80 K. A further increase in temperature above 80 K results in a reversal of the trend; the LE emission starts to quench while the HE emission is enhanced. These temperature changes are progressive. Figure 2 shows a plot of the intensity ratio of the HE/LE bands versus temperature. The luminescence changes for $K_2Na[Ag(CN)_2]_3$ versus temperature are more dramatic than those reported for $Cu_4L_4X_4$ in terms of the reversibility of the process and the energy difference between the two emission bands.

A logical possibility for the luminescence changes around 80 K is a structural phase transition near that temperature. It is conceivable that temperature may alter the distribution of the $[Ag(CN)_2^-]_n$ clusters that differ in n and/or the geometry, which would lead to corresponding changes in the relative intensities of the luminescence bands characteristic of each cluster. Phase transitions have been reported for other dicyanoargentates(I) such as $K[Ag(CN)_2]$, as revealed by pressure-dependent studies (11, 12). To our knowledge, our endeavors for $K_2Na[Ag(CN)_2]_3$ represent the first temperature-dependent studies of structural phase transitions in dicyanoargentate(I) compounds. We have undertaken two parallel approaches to answer the above-mentioned questions. One was based on Raman studies while the other entails direct structural studies by synchrotron X-ray and neutron diffraction methods. The results of our Raman studies have been communicated earlier (1) while the sections below present the detailed results of high-resolution neutron diffraction measurements and a new interpretation of the synchrotron X-ray investigations (1).

4. REINTERPRETATION OF THE SYNCHROTRON X-RAY DATA

Because of the previous diffraction results favoring space group $C2/m$ (1), we reinterpreted the synchrotron X-ray data on $K_2Na[Ag(CN)_2]_3$ as a function of temperature also with this space group in the powder matching mode (9), as it does not require a specific structure model (apart from the space group). To obtain precise lattice parameters, we used the program FullProf (9), based on pseudo-Voigt peak shape with parameters SHAPE1, V and X, two asymmetry parameters (for $2\theta \leq 25^\circ$) and the zero point of the scattering angles $2\theta_0$. The results are summarized in Table 1 and are included in Fig. 5 as a function of temperature. As may be seen from Table 1, the fits (goodness of fit χ^2) are significantly better for space group $C2/m$ (10 parameters) compared to $P\bar{3}1m$ (eight parameters) both at 40 K and at room temperature, in agreement with Ref. (1). Indeed, based on the Hamilton R-ratio test (13), using approximately R_{wp} of Table 1, 287 and 241 trigonal reflections at 40 and 295 K, respectively, we obtain $R_{obs} = R_{wp}(\text{trigonal})/R_{wp}(\text{monoclinic}) = 1.10$ and 1.04 at 40 and 293 K, respectively, compared to $R_{calc} = 1.02$ for both temperatures at a significance level of 0.005.

Finally, we verified the correctness of the structural parameters determined by neutron diffraction (e.g., for 50 K) by refining the 40 K synchrotron X-ray data with these parameters and the lattice parameters from Table 1. This yielded $\chi^2 = 2.99$ and $R_{Bragg} = 0.076$ for 852 reflec-

TABLE 1
Lattice Parameters of $K_2Na[Ag(CN)_2]_3$ as a Function of Temperature, Determined from Synchrotron X-ray Data (1) for Space Group $C2/m$, No. 12

T (K)	a (Å)	b (Å)	c (Å)	β (°)	χ^2	R_{wp}	R_{Bragg}
40	6.91234(9)	11.9919(1)	8.66150(8)	89.946(2)	2.32	15.7	1.39
80	6.9340(1)	11.9917(2)	8.6517(1)	89.964(1)	2.15	16.2	1.63
120	6.94476(9)	12.0309(4)	8.6421(1)	89.990(1)	2.59	19.3	1.41
160	6.9602(1)	12.0721(1)	8.6285(1)	89.959(2)	2.36	15.8	1.48
220	7.00112(8)	12.1091(2)	8.60894(9)	89.971(2)	1.97	15.0	1.30
295	7.0472(1)	12.1886(3)	8.5800(1)	89.975(2)	1.87	14.7	1.17

Note. R_{wp} and R_{Bragg} are the agreement values concerning weighted profile and integrated intensities, repectively (9). Estimated standard deviations (based only on counting statistics, i.e., without error of wavelength determination) are given within parentheses and correspond to the last relevant digit.

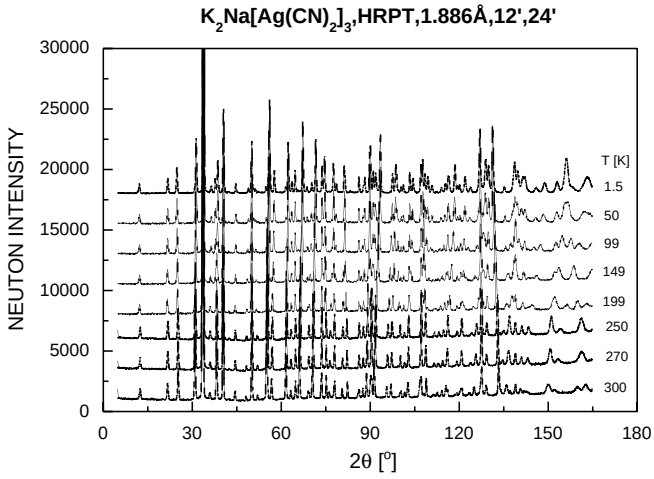

FIG. 3. Temperature dependence of the neutron diffraction pattern of $K_2Na[Ag(CN)_2]_3$.

tions h, k, l, but it was necessary to refine an additional, rather large overall temperature factor, presumably correcting residual errors in the absorption correction.

5. NEUTRON DIFFRACTION INVESTIGATIONS

Figure 3 illustrates the measured temperature dependence of the neutron diffraction pattern of $K_2Na[Ag(CN)_2]_3$. Obviously, there occurs no abrupt structural phase transition as a function of temperature, but in particular the high scattering angle range indicates clearly essential and continuous structural changes. As an example of the refinement results, excellent agreement between observed and calculated neutron intensities is shown in Fig. 4 for the temperature of 1.5 K. Four hundred and eighty-three monoclinic (183 trigonal) reflections (h, k, l) contribute to the neutron diffraction pattern. Corresponding structural parameters are summarized for selected temperatures in Table 2 for the space group $C2/m$. The better fits at low temperatures are due to the considerably reduced thermal atom motions and corresponding higher justification of the use of isotropic temperature factors. Compared to the trigonal structure model (6), which may be used as a first approximation at room temperature ($\chi^2 = 11.7$ and 3.85 at 1.5 and 300 K, respectively), the monoclinic structure with more para-

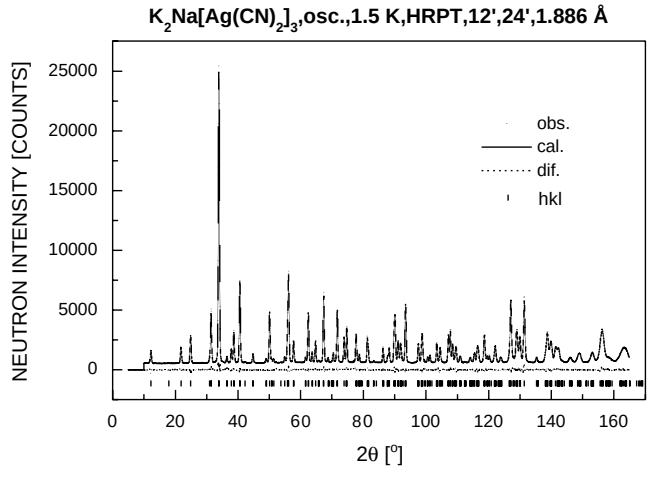

FIG. 4. Observed, calculated (based on space group $C2/m$ with distance constraints) and difference neutron diffraction pattern of $K_2Na[Ag(CN)_2]_3$ at 1.5 K.

TABLE 2

Refined Structural Parameters and Agreement Values of $K_2Na[Ag(CN)_2]_3$ at $T = 1.5$, 99, 199 and 300 K (Lowest Line of Lattice Parameters and Per Atom) for Space Group $C2/m$

a (Å)	b (Å)	c (Å)	β (°)	χ^2	R_{wp}	R_{Bragg}
6.922(1)	11.963(2)	8.666(1)	89.963(1)	2.92	4.82	3.31
6.948(1)	12.007(2)	8.645(1)	89.964(2)	3.10	4.94	5.16
6.996(1)	12.091(2)	8.614(1)	89.970(2)	3.12	4.90	6.84
7.057(1)	12.196(2)	8.584(1)	89.971(3)	3.38	4.63	7.26

Atom	Sites	x	y	z	B (Å^2)
Ag(1)	(2c)	0.5	0	0	0.4(1)
					1.5(3)
					2.1(4)
					4.2(4)
C(1)	(4i)	0.3660(7)	0	0.2121(3)	0.6(1)
		0.365(1)		0.2116(4)	1.0(2)
		0.369(1)		0.2130(5)	1.0(2)
		0.370(1)		0.2124(4)	2.5(2)
N(1)	(4i)	0.2944(6)	0	0.3331(2)	0.79(9)
		0.2937(9)		0.3331(3)	0.9(1)
		0.298(1)		0.3350(4)	2.1(2)
		0.304(1)		0.3374(4)	4.0(2)
Ag(2)	(4e)	0.25	0.25	0	0.34(8)
					1.1(1)
					2.6(2)
					4.1(2)
C(2)	(8j)	0.1842(7)	0.1808(3)	−0.2109(1)	0.42(5)
		0.182(1)	0.1816(5)	−0.2110(2)	1.13(9)
		0.184(1)	0.1794(5)	−0.2098(3)	2.5(1)
		0.179(1)	0.1800(5)	−0.2081(3)	3.3(1)
N(2)	(8j)	0.1496(4)	0.1476(2)	−0.3338(1)	0.54(5)
		0.1486(8)	0.1481(4)	−0.3341(2)	1.33(9)
		0.149(1)	0.1465(3)	−0.3333(2)	2.1(1)
		0.1453(9)	0.1454(3)	−0.3321(2)	3.12(9)
K	(4h)	0	0.332(1)	0.5	0.79(8)
			0.333(2)		1.3(1)
			0.336(2)		1.8(2)
			0.336(2)		2.8(2)
Na	(2e)	0	0	0.5	0.8(1)
					1.1(2)
					2.1(2)
					2.8(2)

Note. The e.s.d's of the lattice parameters include the uncertainty of the wavelength. B = isotropic temperature factor.

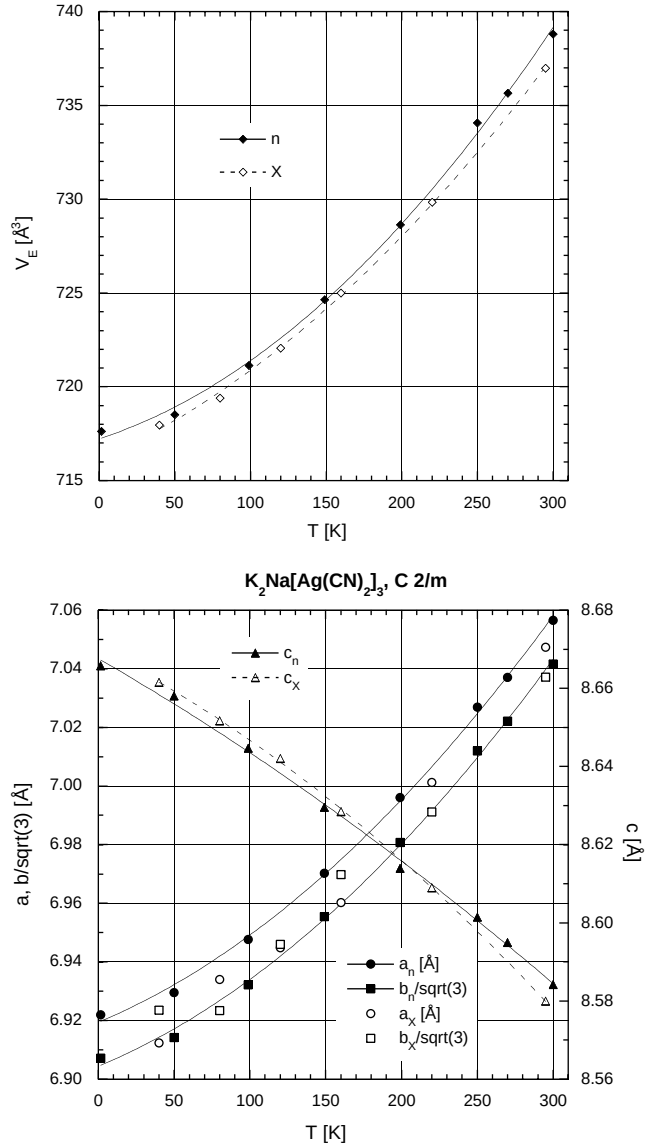

FIG. 5. Unit-cell volume (upper figure) and lattice parameters a, b and c (lower figure) for space group $C2/m$ of $K_2Na[Ag(CN)_2]_3$ as a function of temperature. The lines are polynomial fits of order two. The corresponding errors (e.s.d.'s) are of the order of the symbol sizes.

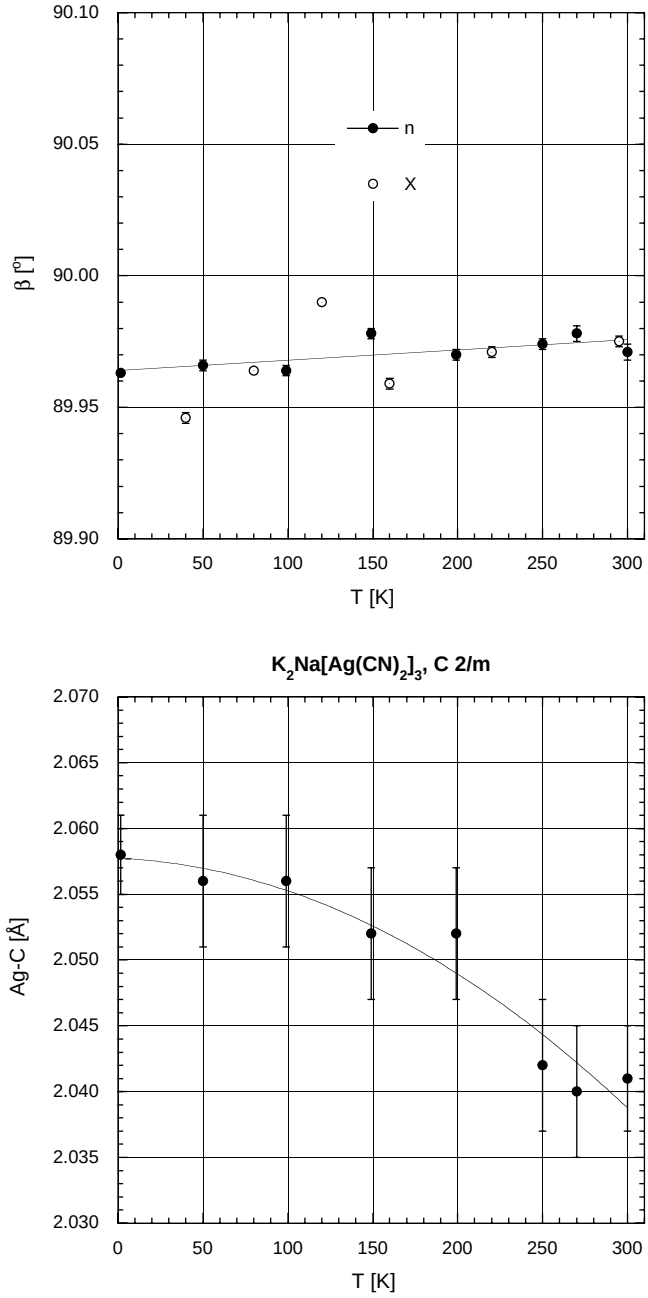

FIG. 6. Temperature dependence of β angle (upper figure) and of Ag–C distance (lower figure, not corrected for thermal motion effects) of $K_2Na[Ag(CN)_2]_3$. The lines are linear and polynomial fits of order two, respectively.

meters yields better fits ($\chi^2 = 2.92$ and 3.38 at 1.5 and 300 K, respectively). Hamilton tests (13) based on R_{wp} ratios, the number of contributing trigonal Bragg reflections (h, k, l) and the number of parameters indicate that the improvement is significant (the monoclinic structure model appears to be valid on the level of significance of less than 0.005). Moreover, the discussed synchrotron X-ray results support the monoclinic structure, which was found to hold for the whole investigated temperature range. Similar results were obtained with the program ZOMBIE, see Table 4, assuming strictly linear N–C–Ag–C–N units. We could not explain the data equally well based on orthorhombic space groups. With linear N–C–Ag–C–N units the only possibility seems to be space group *Cmmm*, but the structure would be disordered.

As shown in Fig. 5, the unit cell volume decreases continuously upon lowering of the temperature, but an anomalous increase of the c-lattice parameter is found with

decreasing temperature, in agreement with Ref. (1). The new neutron results indicate that the lattice parameter a exceeds at all temperatures the lattice parameter $b/\sqrt{3}$. It is interesting to note that both the synchrotron X-ray and the neutron diffraction data indicate that the monoclinic angle β of $K_2Na[Ag(CN)_2]_3$ stays at all temperatures smaller than 90° as shown in Fig. 6.

With respect to the interpretation of the optical properties, it is important to note that there are two inequivalent silver atoms Ag(1) and Ag(2) in the monoclinic structure. The corresponding shortest silver distances Ag(1)–Ag(2) and Ag(2)–Ag(2) are included for selected temperatures in Table 3. In agreement with Ref. (6), Tables 2 and 3 also suggest that the $Ag(CN)_2$ units are only approximately linear (angular deviations from 180° of angle Ag(1)–C(1)–N(1) and of angle Ag(2)–C(2)–N(2) are $\leq 3°$ and $\leq 5°$, respectively. See Table 3). However, with soft distance constraints determined in an iterative way, we keep the chemically reasonable assumption of well defined Ag–C and C–N distances. The refinement showed that practically the same goodness of fit is attained as with the unrestricted refinement (e.g., at 1.5 K: $\chi^2 = 2.90$ unconstrained and 2.92 with distance constraints). Due to essentially increased thermal atom motions at higher temperatures, the bond lengths seem to decrease slightly with increasing temperature, as is shown for Ag–C in Fig. 6 (corresponding corrections were not made). The resulting layer-type structure is illustrated in Fig. 7. As may be seen from Tables 2 and 3 as well as from Fig. 8, the thermal atom vibrations increase considerably in the temperature range from 1.5 to 300 K. To understand further general trends of the structure changes of $K_2Na[Ag(CN)_2]_3$ with temperature, we use the approximation of linear N–C–Ag–C–N molecules. Corresponding results from the program ZOMBIE are given in Table 4 and are illustrated in Fig. 8. The anomalous increase of the c-lattice parameter with decreasing temperature appears to be related to a gradual reorientation of the $Ag(2)(CN)_2$ unit, mainly the angle θ with respect to the c-axis. Presumably, the cause of the different behaviors of θ_1 and θ_2 is related to the different site symmetries $2/m$ and -1 of Ag(1) and Ag(2), respectively.

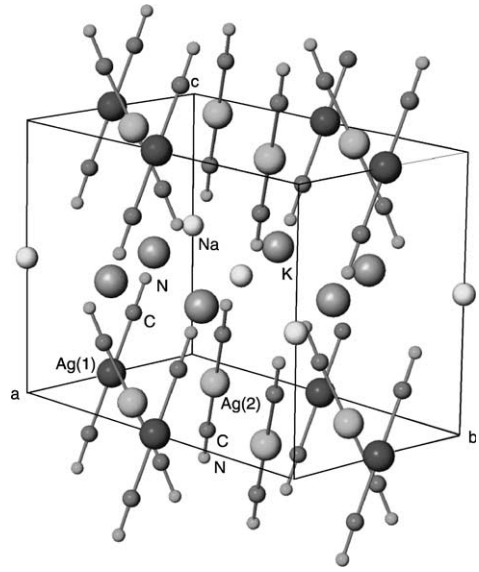

FIG. 7. Monoclinic crystal structure of $K_2Na[Ag(CN)_2]_3$ at 1.5 K, produced by program ATOMS (14). The unit cell is shown by the lines.

6. DISCUSSION AND CONCLUSIONS

The assignment of the two photoluminescence bands of $K_2Na[Ag(CN)_2]_3$ to two $*[Ag(CN)_2^-]_n$ excitons is consistent with the neutron diffraction results. Since two inequivalent Ag atoms were found by fitting the structure to the monoclinic space group $C2/m$, we believe that a luminescent exciton is localized in the environment of each of the two unique Ag atoms. The neutron diffraction results clearly show continuous changes of the monoclinic structure of $K_2Na[Ag(CN)_2]_3$ with no particular changes around 80 K. The earlier Raman results (1) have shown some subtle structural changes above 210 K and preliminary synchroton X-ray and neutron powder diffraction data have indicated small deviations from trigonal symmetry of some lattice parameters around that temperature. However, what is unmistakably clear from both the Raman and structural data is that there are no discrete structural changes in the entire temperature range at which the compound is luminescent ($\leq$ 190 K), definitely not around 80 K where the dramatic luminescence changes are

TABLE 3
Selected Interatomic Distances and Angles of $K_2Na[Ag(CN)_2]_3$ as a Function of Temperature, Calculated from Table 2

T(K)	Ag(1)–Ag(2) (Å)	Ag(2)–Ag(2) (Å)	Ag–C (Å)	C–N (Å)	Ag–N (Å)	Ag(1)–C(1)–N(1) (°)	Ag(2)–C(2)–N(2) (°)
1.5	3.455(1)	3.461(1)	2.058(1)	1.161(1)	3.218(1)	178.5(3)	176.1(2)
99	3.468(1)	3.474(1)	2.056(1)	1.161(1)	3.216(1)	178.0(4)	176.1(3)
199	3.492(1)	3.498(1)	2.051(1)	1.162(1)	3.212(1)	178.5(5)	175.3(3)
300	3.523(1)	3.528(1)	2.041(1)	1.170(1)	3.210(1)	176.8(5)	175.6(3)

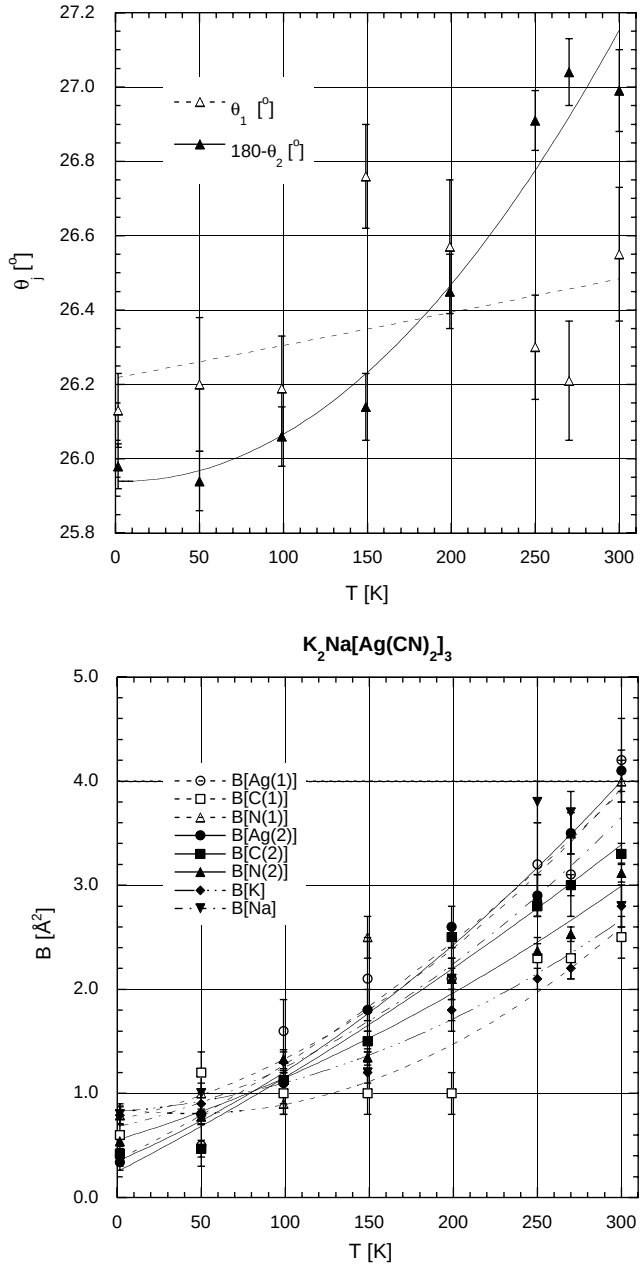

FIG. 8. Temperature dependence of θ angles of the linear $Ag(1)(CN)_2$ and $Ag(2)(CN)_2$ units (upper figure) and of the isotropic temperature factors (lower figure) of $K_2Na[Ag(CN)_2]_3$. The lines are linear and polynomial fits of order two, respectively.

observed. After ruling out several other possibilities, we arrive at the conclusion that the luminescence changes with temperature are attributed to corresponding changes in the energy transfer pathways between the two luminescent excitons. A detailed photophysical study of the electronic structure of $K_2Na[Ag(CN)_2]_3$ will be published elsewhere and that study will include qualitative and quantitative characterization of the energy transfer processes in the compound as well as an assessment of the various alternative assignments of the luminescent excited states. The conclusion is that normal energy transfer pathways (from the HE to LE exciton) are responsible for the changes between 10 and 80 K. Above 80 K, the thermal energy is large enough such that a back energy transfer process takes place from the LE to the HE exciton.

TABLE 4

Angle θ_1 and Angle θ_2 of Linear $Ag(1)(CN)_2$ and $Ag(2)(CN)_2$ Units with Respect to the *c*-Axis for $K_2Na[Ag(CN)_2]_3$ as a Function of Temperature, as Calculated by the Program ZOMBIE (10)

T (K)	θ_1 (°)	θ_2 (°)	χ^2
1.5	26.1(1)	154.02(6)	9.46
99	26.2(1)	153.94(8)	8.20
199	26.6(2)	153.6(1)	7.67
300	26.6(2)	153.0(1)	7.27

ACKNOWLEDGMENTS

Support of the neutron diffraction investigations by the Laboratory for Neutron Scattering, ETHZ & PSI and by SINQ is gratefully acknowledged. Acknowledgement is also made to the donors of the Petroleum Research Fund, administrated by the American Chemical Society, for the support of this research to H. H. P. and the Robert A. Welch foundation for supporting the contribution of M.A.O.

REFERENCES

1. C. L. Larochelle, M. A. Omary, H. H. Patterson, P. Fischer, F. Fauth, P. Allenspach, B. Lucas, and P. Pattison, *Solid State Commun.* **114,** 155 (2000).
2. (a) H. D. de Ahna and H. D. Hardt, *Z. Anorg. Allg. Chem.* **387,** 61 (1972); (b) H. D. Hardt and H. Gechnizdjani, *Z. Anorg. Allg. Chem.* **397,** 23 (1973); (c) H. D. Hardt and A. Pierre, *Z. Anorg. Allg. Chem.* **402,** 107 (1973); (d) H. D. Hardt and A. Pierre, *Inorg. Chim. Acta* **25,** L59 (1977); (e) D. D. Hardt and H. J. Stoll, *Z. Anorg. Allg. Chem.* **480,** 193 (1981); (f) D. D. Hardt and H. J. Stoll, *Z. Anorg. Allg. Chem.* **480,** 199 (1981).
3. (a) K. R. Kyle, C. K. Ryu, J. A. DiBenedetto, and P. C. Ford, *J. Am Chem. Soc.* **113,** 2954 (1991); (b) K. R. Kyle, J. A. DiBenedetto, and P. C. Ford, *J. Chem. Soc., Chem. Commun.* 714 (1989); (c) K. R. Kyle and P. C. Ford, *J. Am Chem. Soc.* **111,** 5005 (1989); (d) K. R. Kyle, W. E. Palke, and P. C. Ford, *Coord. Chem. Rev.* **97,** 35 (1990); (e) A. Døssing, C. K. Ryu, S. Kudo, and P. C. Ford, *J. Am Chem. Soc.* **115,** 5132 (1993); (f) P. C. Ford, *Coord. Chem. Rev.* **132,** 129 (1994); (g) D. Tran, C. K. Ryu, and P. C. Ford, *Inorg. Chem.* **33,** 56 (1994); (h) J. A. Simon, W. E. Palke, and P. C. Ford, *Inorg. Chem.* **35,** 6413 (1996); (i) M. Vitale, W. E. Palke, and P. C. Ford, *J. Phys. Chem.* **96,** 8329 (1992); (j) M. Vitale, C. K. Ryu, W. E. Palke, and P. C. Ford, *Inorg. Chem.* **33,** 561 (1994); (k) P. C. Ford and A. Vogler, *Acc. Chem. Res.* **26,** 220 (1993).
4. A. Burini, R. Bravi, J. P. Fackler, Jr., R. Galassi, T. A. Grant, M. A. Omary, B. R. Pietroni, and R. J. Staples, *Inorg. Chem.* **39,** 3158 (2000).

5. M. A. Rawashdeh-Omary, M. A. Omary, G. E. Shankle, and H. H. Patterson, *J. Phys. Chem. B* **104,** 6143 (2000).
6. M. Zabel, S. Kühnel, and K.-J. Range, *Acta Crystallogr. C* **45,** 1619 (1989).
7. P. Fischer, B. Lucas, H. H. Patterson, and C. L. Larochelle, *Appl. Phys. A* (2002), accepted for publication.
8. P. Fischer, G. Frey, M. Koch, M. Könnecke, V. Pomjakushin, J. Schefer, R. Thut, N. Schlumpf, R. Bürge, U. Greuter, S. Bondt, and E. Berruyer, *Physica B* **276-278,** 146 (2000).
9. J. Rodriguez-Carvajal, *Physica B* **192,** 55 (1993).
10. (a) P. G. Byrom, S. E. Hoffmann, and B. W. Lucas, *J. Appl. Crystallogr.* **22,** 629 (1989); (b) P. G. Byrom and B. W. Lucas, *J. Appl. Crystallogr.* **24,** 1005 (1991).
11. D. M. Adams and P. A. Fletcher, *Spectrochim. Acta A* **44,** 437 (1988).
12. P. T. T. Wong, *J. Chem. Phys.* **70,** 456 (1979).
13. W. C. Hamilton, *Acta Crystallogr.* **18,** 502 (1965).
14. E. Dowty, "Program ATOMS, Shape Software." 521 Hidden Valley Road, Kingsport, TN 37663, USA.